LA-UR -91-2816

LA-UR--91-2816

DE91 018003

TITLE: CHARACTERIZATION OF NONLINEAR INPUT-OUTPUT SYSTEMS USING TIME SERIES ANALYSIS

AUTHOR(S): Norman F. Hunter and James Theiler

SUBMITTED TO: 1st Experimental Chaos Conference, Arlington, VA, October 1-3, 1991

Received by OSTI

0 5 1991

Los Alamos

Los Alamos National Laboratory
Los Alamos, New Mexico 87545

FORM NO. 836 R4
ST. NO. 2629 5/81

CHARACTERIZATION OF NONLINEAR INPUT-OUTPUT SYSTEMS USING TIME SERIES ANALYSIS

NORMAN HUNTER
Dynamic Testing Section,
Group WX-11,
Los Alamos National Laboratory, Los Alamos, NM 87545, USA

and

JAMES THEILER
Theoretical Division and Center for Nonlinear Studies,
Los Alamos National Laboratory, Los Alamos, NM 87545, USA

ABSTRACT

Data obtained from time series analysis has been used for a number of years for the characterizaton and response prediction of linear sytems. This paper describes a time series technique for the analysis of nonlinear systems through the use of embeddings using delay coordinates or appropiate transformations of delay coordinates (local singular value decomposition or local canonical variate analysis). Local linear approaches are used to characterize the state evolution. Application of the technique is illustrated for a single degree of freedom oscillator with nonlinear stiffness, a mechanical chaos beam, and a climatic data time series. In each application analysis from measured data is emphasized. State rank, lyapunov exponents, and expected iterated prediction errors are quantified. The technique illustrated should be useful in the analysis of many forms of experimental data, especially where the state rank is not excessively large.

1. Model Theory

Consider a system where the input and response time series are sampled with sample interval τ. Using an extension of Taken's theorem [3]an image of the state is Duffingoscillator [3] have been reported in the literature. constructed using delay coordinates.

$$y(t) = f\{y(t-\tau), y(t-2\tau), \ldots y(t-j\tau), u(t), u(t-\tau), u(t-2\tau), \ldots u(t-l\tau)\} \quad (1)$$

For a linear system, this formulation reduces to a linear combination of inputs and responses (ARMA model). A fundamental problem in applying this technique to nonlinear systems is in the determination of the proper functional form to use in Eq. 1. While numerous global functional forms may be used (polynomials, radial basis functions, etc), an efficient means of selecting a proper functional form is through the use of local techniques. Using points in the neighborhood of the state for which prediction is desired we use a locally linear , but globally nonlinear model.

1.1. Embedding Techniques

Our image of the state space in equation Eq. 1 is formed in a space where each coordinate is one of the delayed $u(t)$ or $y(t)$ terms. The dimension of the space is effectively $j + l$, or the number of input terms plus the number of response terms, possibly plus a constant term. This is often a very inefficient representation of the system state, with a dimension larger than is required. We have used two approaches to alleviate this dimensionality problem, local local principal component analysis and local canonical variate analysis. Both approaches provide an estimate of the number of effective states using coordinates which are formed from a local linear combination of the delay coordinates. The singular value decomposition technique is applied primarily to autonomous systems , and the canonical variate analysis technique to driven systems.

1.2. Iterative Prediction

The prediction of a given value $y(t+1)$ from past values of $y(t)$ and $u(t)$ is useful but for many purposes incomplete, as we often desire to predict future response waveforms consisting of many individual sample intervals. To achieve this form of prediction we iteratively predict the response, using successive $y(t)$'s as past values of the response as they are computed. First our model is applied to solve for $y(t_0 + \tau)$. The $y(t_0)$ computed serves as an input to a succeeding model, which solves for $y(t_0 + \tau)$ These "iterative" predictions are repeated many times for succesively increasing multiples of t to obtain the estimated response waveshape over long time periods. All of the predictions illustrated in this paper are iterated predictions.

1.3. System Characterization

The system is characterized based on the parameters which are obtained from our local linear models. An estimate of state rank, derived from the number of significant singular values, an estimate of linearity or nonlinearity derived from the successive locations of the system poles, the iterated prediction, and estimates of error growth are obtained from the model

2. Applications

While the techniques illustrated in this paper are applicable to autonomous systems, we emphasize their application to driven systems. Driven systems occur in a wide variety of disciplines, including physics (mechanical vibrations), biology (population equations), and meteorology (climatic records). We discuss input output modeling for three oscillatory physical systems: the first is a duffing like oscillator excited by band limited random noise, the second is a mechanical beam moving in a magnetic double potential well, and the third is the long term variation in global ice volume (characteristic of the ice ages). In the first case, evidence for nonchaotic behavior is presented; in the second case, chaotic behavior clearly occurs; in the third case, the irregular motion is found to be nonchaotic. In addition to the illustrated examples, we have applied this technique to single and multi- degree of freedom linear oscillators (using digitally simulated data), multi-degree of piecewise linear oscillators (using digitally simulated data), single-degree-of-freedom hysteretic oscillators (using digitally simulated data), and a six degree of freedom mechanical test system (using data acquired during a structural vibration test). Additional examples using various functional forms, including applications to a heat exchanger system [1], ship rolling [2], a Van DerPol Oscillator [2], have been reported in the literature.

/subsectionAnalog Duffing Oscillator As a generic example of a system driven by an input acceleration, we consider the following Duffing-like [1] oscillator of Eq. 2.

$$y" + 2\zeta\omega_n(y' - y_0') + \omega_n^2(y - y0) + \alpha\omega_n^2(y - y0)2 + \beta\omega_n^2(y - y0)|y - y0| = 0 \quad (2)$$

The input is the acceleration $y_0"$ [2] $y_0"$ and the response is $y"$. Here, ω_n is the natural frequency of the linear restoring force, ζ is the damping coefficient, and α and β are the coefficients of the antisymmetric and symmetric nonlinear restoring forces. The behavior exhibited by a driven Duffing system is characteristic of many of thenonlinearities encountered in practice, especially those behaviors encountered in strongly oscillatory systems with relative low energy dissipation (damping).

Figure Fig. 1 compares the iterated prediction and measured response of the nonlinear time series model for this case of the strongly nonlinear driven Duffing oscillator. Seven thousand training points were used to formulate this local linear model,which is significantly superior to the best linear model we found. The average iterated prediction error is computed over a range of 300 samples (about 2.5 seconds) and found to be 0.62 for the best linear model and 0.32 for the nonlinear (in this case, local linear) model. The local state rank of the system consistently ranges from three to four, indicating that relatively few state variables are required to model the system. As we succesively model different sections of the time series the pole locations of the local linear model vary drastically with time, indicating the presence of a strong nonlinearity.

In this particular example, we hypothesize that this particular Duffing oscillator, driven by this particular input sequence, is essentially nonchaotic, since a reasonable long term prediction is apparently possible. To quantify the accuracy of long term predictions, the two separate effects described in the theory section must be considered, the effective lyapunov exponent of the system, and the potential effects of the accumulation of errors in the delayed terms used in estimating the state of the system. Figure Fig. refduffling err illustrates the propagation of an infinetisimal error

---

[1] The Duffing oscillator is usually written as a differential equation with a cubic term. Here,to simplify the analog circuitry, we use $y|y|$ instead of y^3, which although not cubic, does preserve the antisymmetric nature of the cubic nonlinearity

[2] Although the term $y0''$ does not explicitly appear in equation Eq. refduffling, successive integration of $y0''$ determines $y0'$ and $y0$ and these do appear.

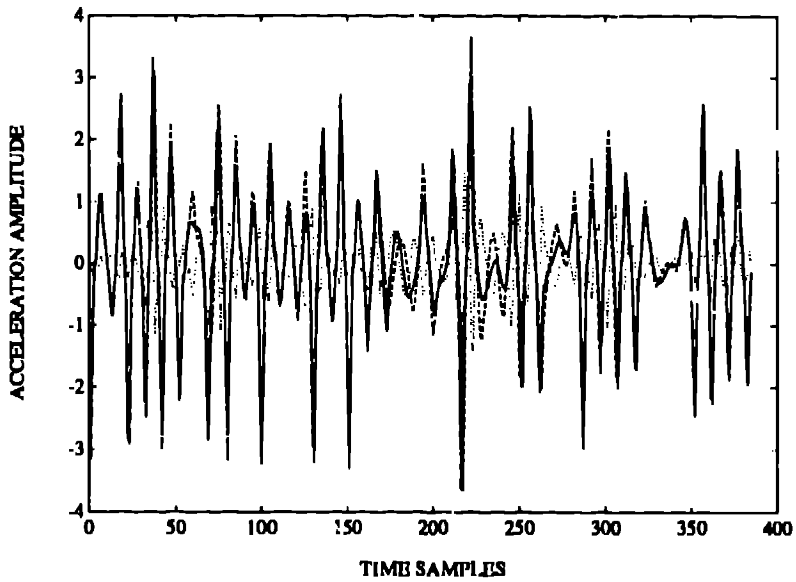

Figure 1: *Response Time Histories for a Strongly Nonlinear Duffing Oscillator (Measured Data), the Corresponding Nonlinear model(Iterated Prediction- - - - -), and the (Error ....)*

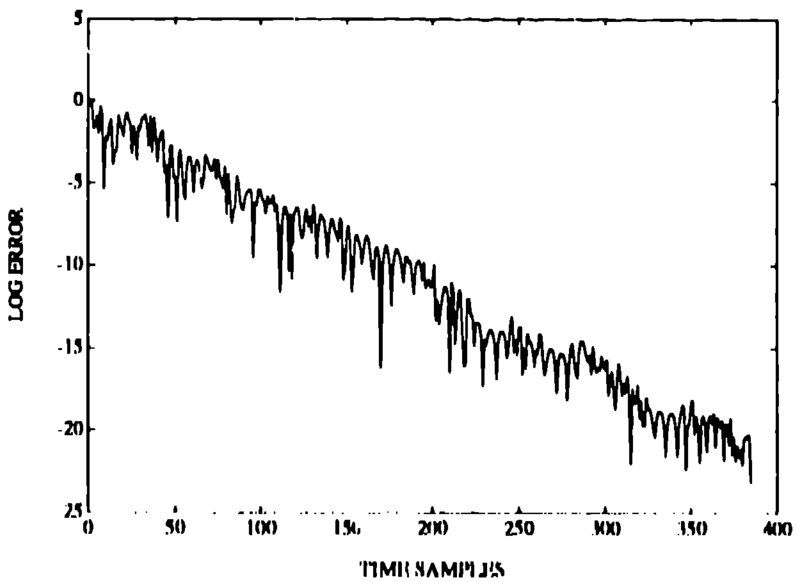

Figure 2: *Error Propagation for the Nonlinear Duffing Oscillator, Assuming an Infinitisimal Error at the Start of the Iterated Prediction Range.*

The propagation of the error clearly illustrates the effect of a negative lyapunov exponent. In contrast, the iterated prediction error grows and decays in a complex manner

For chaotic systems, even approximate long term prediction is usually impossible, however, for input-output systems, depending on how directly the response depends on the input, iterated predictions can sometimes give quite reasonable results. The example in the next section is a case for which long term prediction of the system response is not possible.

2.1. Beam moving in a double potential well

As our next illustration of the application of nonlinear time series analysis to driven systems we choose a system which is clearly exhibiting chaotic behavior, the "chaos beam" described by Moon [4]. In this example, discussed in detail by Hunter [5], an experimental oscillator was built which exhibited chaotic transitions between two stable states. Measured acceleration and strain data from this system constitute the input and output time series.

Typical predicted and measured response time series for this system are shown in Figure Fig. [redacted] 3. Unlike the case in the previous section, chaotic behavior of the system leads the predicted and measured response to rapidly diverge. The iterated prediction error is essentially unity.

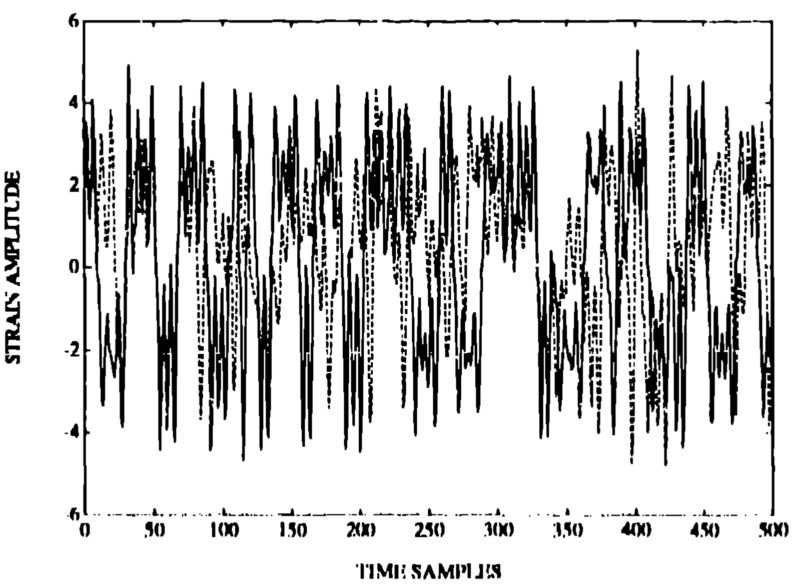

Figure 3: *Time history of the measured and iterated model predictions for the chaos beam.*

As in the previous case of the Duffing Oscillator the model indicates a local state rank of three to four. As we sweep through the model a drastic variation in the location of the model poles occurs, indicating a strongly nonlinear system. The variation in the pole locations changes in a manner different from that in the Duffing Oscillator case and there is the possibility that this variation in pole locations may be used to characterize the form of the nonlinearity.

We examine the error growth rate for this model of chaos beam behavior and quantify the results in Fig. ref.chaos-errs. In contrast to the Duffing Oscillator illustrated above, it is clear that the error growth rate implies a chaotic system with a positive lyapunov exponent. The estimated iterative prediction error is dominated by the effect of the positive lyapunov exponent until the errors reach values near the mean value of the time series itself. At this point the effective error saturates. For this system, long-term iterated forecast error provides a poor measure of model validity. Even for a very good model, small errors will grow exponentially in time. The model will be incapable of predicting which well the beam will be in at some time far in the future. However, part of what is desired from an input- output model is knowledge of how the response will depend on the input in terms of various statistical averages. Figure Fig. 5 shows the power spectra of iterated and measured response time series. Although the model is not good at making long-term forecasts of the specific time history response, it does successfully predict the power spectrum.

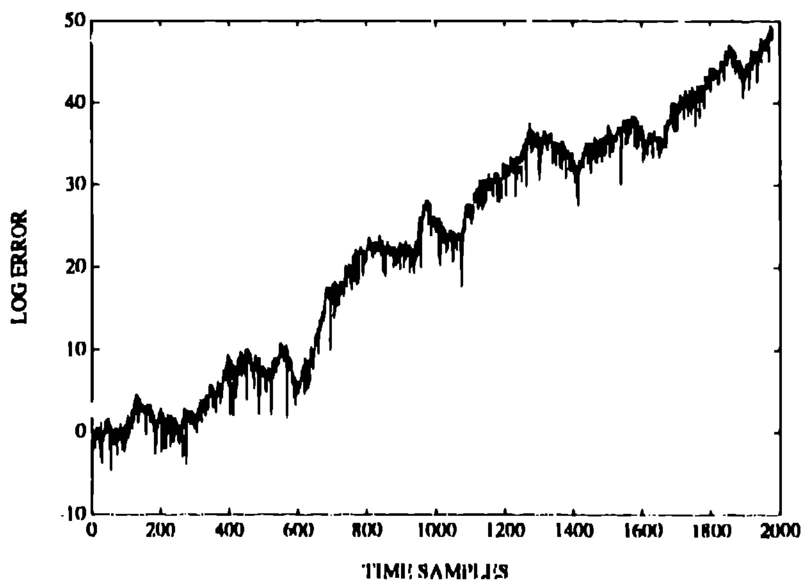

Figure 4: *Growth of an Infintesimal Error Over The Time Range Illustrated.*

2.2. *Climatic Data Time Series*

As another example of the nonlinear modeling of input output time series, we consider an application involving long term climatic data, specifically the long term, rather

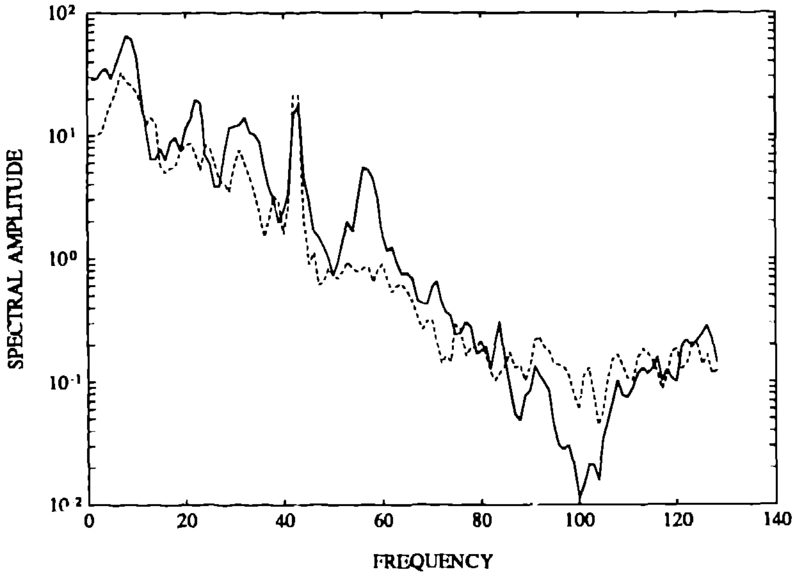

Figure 5: *Measured Response Spectrum ( ) and Model Spectrum (- - -)*

complex variation of global ice volume. The modeling of a geologically derived time series presents a difficult problem, since geologic time series are often noisy, and event timing may be uncertain.

The total solar energy incident on the upper atmosphere over a 24 hour period varies with time of day, latitude, and season. Changes in the tilt of the earth's axis (obliquity), the season in which the Northern hemisphere is tilted most away from the sun (precession) and in the shape of the earth's orbit (eccentricity) change the effective solar energy received in a given month at a given location. Over millennia the energy received from the sun, termed solar insolation, varies about 20 percent at latitudes above 45 degrees North. Figure In 1941, Milkanovich postulated that the summer insolation at relatively high northern latitudes was a determining factor in the evolution of the ice ages. Winters at these latitudes are always cold enough for snow to accumulate. A critical factor in the development of ice sheets is summer melting, as consistent incomplete summer melting leads to ice sheet growth. Recently Imbrie *et al.* [6, 7] showed that common frequency components with periods characteristic of precession, whose period is 21,000 years, and obliquity, whose period is 41,000 years, are strongly present in the ice volume time series illustrated in Figure Fig. 6. They also pointed out that the dominant component in the ice volume time series, whose period is 95,000 years, is absent from the solar insolation time series.

While components with a 95,000 year period are absent from the insolation time series, they are present in the envelope of the series. A dominant variation in eccentricity, with a period of about 100,000 years. modulates insolation signal, causing regions of low variance to occur about every 100,000 years. It is our contention that regions of low variance in the insolation signal correspond to glacial periods.

Using our modeling process, we apply the methods of time series analysis [?] to the insolation and ice volume time series. A systematic search of possible nonlinear and linear models was made for data from two ocean cores, V28-238 and V28-239. A cross validation procedure based on successively selecting segments of the ice volume time series for prediction, while training on the remainder of the series, was used. Iterated predictions over a period of about 90,000 years were made, sufficient to predict about one ice age into the future. These results were compared to those obtained using simulated insolation and ice volume time series whose power spectra were identical to those of the actual time series but with randomized phases. Nonlinear models, and in a few cases, linear time series models, gave results whose average iterated prediction errors were between three and five sigma below those obtained for the simulated time series. The best models were nonlinear. 20 lagged values of solar insolation (about 60,000 years) were used for the model input and between 4 and 20 lagged ice volume values (12,000 to 20,000 years) as lagged response values. Local singular value decomposition indicated that the solar insolation-ice volume system has approximately three significant state variables.

Since solar insolation data are available for the future, nonlinear forecasting techniques can be applied to predict the next ice age. For this prediction eccentricity tuned data was used from core V28-239. Except for the last 60,000 years, the entire past insolation and ice volume data sets were used for training. In Figure Fig. 6, measured and predicted ice volume for the last 150,000 years are compared. Continued iteration of the model is then used to predict a future peak in global ice volume, occurring, as shown in Figure Fig. 6, in about 40,000 years.

3. Conclusions and Future Work

We have illustrated a method for the analysis of nonlinear systems which makes use of a segment of the input and response waveforms for the system (training data) to build a system model. This model provides, through geometry of the pole locations in the z plane, an estimate of the degree of nonlinearity of the system. Error growth rate and iterated prediction errors are estimated. Future time series responses of the system under study are predicted. Further application of this model formulation to a greater variety of nonlinear systems is planned. Some features of the model include:

1. Training data used must explore the same regions of the state space as those for which response prediction is desired. Extrapolation to unexplored regions of the state space is limited. 2. The number of significant singular values gives an estimate of the state rank of the system. 3. The algorithm gives an indications of regions of the state space where prediction may be difficult.

At this point the technique looks promising for the detection of nonlinearity in dynamic systems and for the prediction of the time series response (for non chaotic regions) or the response statistics (for chaotic regions). The use of this technique is not limited to data from mechanical oscillators but may be applied to a wide variety

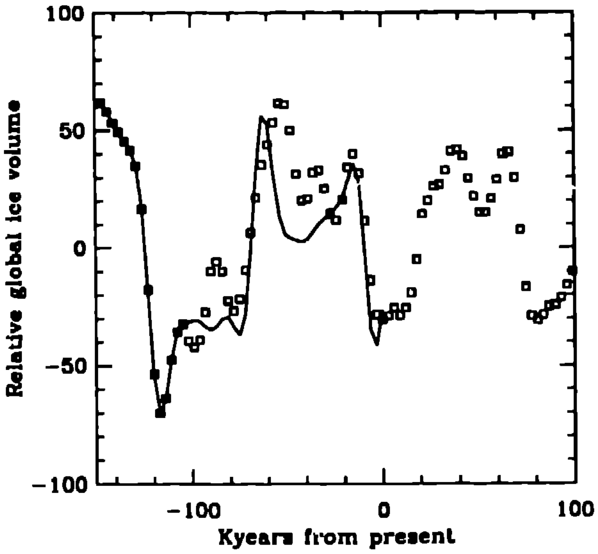

Figure 6: *Prediction of the next ice age, assuming no human-induced effects. Shown are the ice age data up to the present (—), and the iterated predictions (□) starting from about 150,000 years in the past and continuing into the future.*

of systems of low to moderate state rank where input and response time series are available.

4. Acknowledgements

We are grateful to Martin Casdagli, Doyne Farmer, Stephen Eubank, and John Gibson for useful discussions.

This work was partially supported by the National Institute for Mental Health under grant 1-R01-MH47184-01, and performed under the auspices of the Department of Energy. We urge the reader to use these results for peaceful purposes.

5. References

1. S. A. Billings, K. M. Tsang, and G. R. Tomlinson, "Application of the narmax method to nonlinear frequency response estimation," in *Proceedings of the 6th International IMAC Conference* (1987).
2. Lai, "Threshold modelling of nonlinear dynamic systems," in *Proceedings of the 5th International Modal Analysis Conference* (1987).
3. M. Casdagli, D. D. Jardins, S. Eubank, J. D. Farmer, J. Gibson, N. Hunter, and J. Theiler, "Nonlinear modeling of chaotic time series: theory and applications," in *EPRI Workshop on Applications of Chaos* (1991). To appear.
4. F. Moon, *Chaotic Vibrations*. (Wiley, 1987), p. 280.

5. N. F. Hunter, "Pleistocene climate as a dynamic system," in *Nonlinear Prediction and Modeling*, M. Casdagli and S. Eubank, eds. (Addison-Wesley, 1991). To appear.
6. J. Imbrie and N. J. Shackelton, "Variations in the earth's orbit: Pacemaker of the ice ages," *Science* **194**, 1121-1132 (1976).
7. J. Imbrie and J. Z. Imbrie, "Modeling the climatic response to orbital variations," *Science* **207**, 943–952 (February, 1980).
8. M. Casdagli, "A dynamical systems approach to mod[illegible]ling driven systems," in *Nonlinear Prediction and Modeling*, M. Casd[illegible]nd S. Eubank, eds. (Addison-Wesley, 1991). To appear.